Lasers in Medical Science (2023) 38:221
https://doi.org/10.1007/s10103-023-03883-2

ORIGINAL ARTICLE

Effect of photobiomodulation on the behaviour of mesenchymal stem cells in three-dimensional cultures

Ana Laura Martins de Andrade[1,2] · Lucília Pereira da Silva[3,4] · Nivaldo Antonio Parizotto[1,2] · Patrícia Brassolatti[5] · Richard Eloin Liebano[1] · Alexandra Pinto Marques[3,4]

Received: 6 June 2023 / Accepted: 13 September 2023 / Published online: 25 September 2023

Abstract

Photobiomodulation (PBM) has been proposed as a strategy to improve the regenerative capacity of human adipose-derived stem cells (hASCs). Yet, this effect has been proved in 2D culture conditions. To analyze the effect of different doses of laser irradiation (660 nm) with different levels of energy (1 J, 2 J and 6 J) on hASCs cultured at 2D and 3D conditions. We used gellan gum spongy-like hydrogels as a biomaterial to 3D culture hASCs. Different doses (1–7 daily irradiations) and energy levels (1-6 J) of PBM were applied, and the metabolic activity, viability, proliferation, and release of ROS and IL-8 was evaluated up to 7 days. In 3D, cell proliferation increased at high energy (6 J) and after a single dose of irradiation, while in 2D, metabolic activity and proliferation was enhanced only after 3 doses and independently of the energy. More than 1 dose was needed to promote ROS secretion both in 2D and 3D culture conditions. Interestingly, a decrease of IL-8 secretion was detected only in 3D after 3–7 daily irradiations. Overall, hASCs response to PBM was not only dependent on the energy level and the number of applied stimuli, but also on the in vitro culture conditions.

Keywords Low-level laser therapy · Stem cells · Cell culture techniques

Introduction

Laser photobiomodulation therapy (PBM) is being used for the treatment of several clinical dysfunctions, with emphasis on cutaneous wound healing. The application of PBM has shown to promote increased cell activity and trophic-regeneration through the modulation of the inflammatory response [1–3]. The effect of PBM in vitro was particularly reflected on increased mitochondrial respiration and ATP production [4, 5], synthesis of proteins [6], and cell migration and proliferation [3, 7, 8].

The potential of PBM is being spanned to the tissue engineering and regenerative medicine (TERM) field due to its ability to modulate mesenchymal stem cells (MSCs) behavior. PBM has been shown to increase MSC proliferation without altering stem cells potential [9, 10]. However, the outcomes that are being reported present large discrepancies due to the lack of standard protocols [11–13]. Moreover, these studies have been performed in flat and rigid two-dimensional monolayers (2D) that receive homogeneous amount of nutrients and growth factors from the medium, which does not reflect the in vivo situation [14, 15].

✉ Nivaldo Antonio Parizotto
nivaldoaparizotto@hotmail.com

1 Physiotherapeutic Resources Laboratory, Post-Graduate Program in Physiotherapy, Department of Physiotherapy, Federal of University São Carlos, São Carlos, São Paulo, Brazil

2 Post-Graduate Program in Biomedical Engineering, Department of Biomedical Engineering, University Brazil, Campus Itaquera, Rua Carolina Fonseca, 584, Vila Santana, 08230030, São Paulo, SP, Brazil

3 3B's Research Group, Biomaterials, Biodegradable and Biomimetics, Avepark, Parque de Ciência e Tecnologia, Zona Industrial da Gandra, 4805-017 Barco, Guimarães, Portugal

4 ICVS/3B's - PT Government Associate Laboratory, 4805-017 Braga, Guimarães, Portugal

5 Department of Morphology and Pathology, Post-Graduate Program in Evolutionary Genetics and Molecular Biology, Federal University of São Carlos (UFSCar), São Carlos, São Paulo, Brazil

Previous studies have shown that tridimensional (3D) culture models provide a better recreation of the in vivo-like environment, allowing the cells to migrate and establish communication among themselves and with the extracellular matrix (ECM) [16]. Hydrogels present high similarities with the native ECM owing to their high water content and viscoelastic features. Moreover, hydrogels can be engineered to recreate cell microenvironments and construct bio-artificial cell niches, hence showing remarkable features to be used as 3D culture models [16]. Recent studies have shown the potential of hydrogels based on the bacterial exopolysaccharide gellan gum (GG) to be used for different TERM applications [17–19]. In particular, GG-based spongy-like hydrogels have shown superior mechanical performance and flexibility and intrinsic cell adhesion features, not observed in the precursor hydrogels [19]. In this context, it was hypothesized that GG spongy-like hydrogels would provide an improved environment in relation to 2D culture surfaces, to study the effect of PBM on MSCs derived from the adipose tissue (ASCs). Motivated by our previous results evidencing a positive effect of PBM over hASCs in 3D [8], in this work we aimed to analyze the effect of single and multiple doses of laser irradiation (660 nm) with different levels of energy (1 J, 2 J and 6 J) on hASCs cultured at 2D and 3D conditions. Moreover, the mechanism of action of this therapy was evaluated in order to establish the conditions that can be safely and efficiently applied in future in vivo studies.

Material e methods

Photobiomodulation (PBM)

A red laser, aluminum gallium indium phosphide diode (InGaAIP) (Therapy XT, DMC São Carlos/SP, Brazil) with a wavelength of 660 nm (nm), power of 40 mW, beam transversal area of 0.0475 cm^2, and energies of 1 J, 2 J and 6 J (Table 1) was used in the experiments established according to a procedure previously described [8]. The laser pointer was perpendicularly directed to each well and kept fixed, with a distance of 3.34 cm from the laser pen to the bottom of the well or the top of the scaffolds; this distance allowed the laser beam to cover the total area of the well, the form of application of the non-contact laser in cells, with this distance, followed descriptions in the literature. [8]. A power meter was used to verify the laser power before and after irradiations.

Preparation of gellan gum spongy-like hydrogels

GG spongy-like hydrogels were prepared according to a procedure previously described and patented with some modifications [19]. GG (Sigma-Aldrich, Portugal) was first modified with divinyl sulfone (DVS, Sigma-Aldrich, Portugal) as previously reported [20]. The efficiency of DVS conjugation was confirmed by ^{1}H-NMR. GG-DVS (1%, w/v) was then reacted with CGRGDSP peptide (800 µM, 95% purity, Selleckchem, USA) for 1 h at RT. The efficiency of CGRGDSP peptide conjugation was determined by micro-BCA. GG solution (2%, w/v) was dissolved at 90ºC for 30 min and then mixed with the GG-DVS-RGD solution (1%, w/v) at RT (1:1, v:v). The mixture was poured into a petri dish and left to crosslink at RT. Hydrogels were then frozen at -80 ºC, for 24 h and lyophilized (LyoAlfa 10/15, Telstar, Spain) for three days to obtain the dried polymeric structure. The microstructural, physical–chemical and mechanical properties of the spongy hydrogel are shown in Fig. 1. Discs of 5 mm diameter and 4 mm of height were punched and used for the cell culture.

Table 1 Parameters of the PBM irradiation

Parameters	Values
Power (mW)	40
Wavelength (nm)	660
Mode of Action	Continuous
Beam Transverse Area (cm^2)	0.0475
Irradiance (W/cm^2)	0.84
Energy Density (J/cm^2)	21; 42; 126
Time (s)	25; 50; 150
Energy (J)	1; 2; 6
Number and Frequency of Sessions	7 irradiations (every 24 h)

Microstructural characterization of gellan gum spongy-like hydrogels

A high-resolution X-Ray Microtomography System Skyscan 1072 scanner (Skyscan, Kontich, Belgium) was used to analyze the microstructure of the dried GG structures. Samples were scanned in a high-resolution mode using a pixel size of 23.3 mm and integration time of 1.7 s. The X-ray source was set at 35 keV of energy and 215 µA of electric current. Representative data sets of 150 slices were transformed into a binary picture using a dynamic threshold of 45e255 (grey values) to distinguish the polymeric material from pore voids. This data was used for morphometric analysis (CT Analyzer v1.5.1.5, SkyScan) which included quantification of the pore wall thickness, structure porosity and pore size. 3D virtual models of representative regions in the bulk of the materials were created, visualized and registered using the image processing software (CT-vox, SkyScan).

A

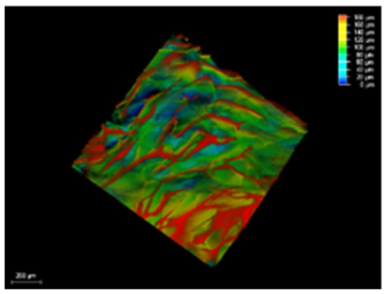

B

Porosity[1] (%)	94.78 ± 1.22
Pore size[1] (µm)	128.08 ± 17.24
Pore wall thickness[1] (µm)	11.84 ± 0.45
Water content[2] (%)	2022 ± 314
Compressive modulus[2] (kPa)	73.20 ± 24.34

Fig. 1 Gellan gum spongy-like hydrogels microstructural, physic-chemical and mechanical properties. **A** Microstructure of gellan gum spongy-like hydrogels, determined by confocal microscopy. **B** Summary of gellan gum spongy-like hydrogels microstructural, physic-chemical and mechanical properties ([1] determined by micro-CT; [2] determined after swelling for 48 h). Data results from at least 3 independent experiments

A Leica TCS SP8 confocal microscope (Leica, Germany) was used to analyze the microstructure of wet samples after staining with the fluorescent dye 4',6-diamidino-2-phenylindole (DAPI, 0.2 mg/mL, Biotium, USA).

Water content of gellan gum spongy-like hydrogels

The water content was determined by measuring the weight of the dried GG samples before (Wd) and after (Ww) immersion into α-Minimum Essential Medium (α-MEM) medium at 37ºC for 2 days, to ensure full saturation.. The water content was determined using the following equation.

$$\text{Water content}(\%) = (\text{Ww} - \text{Wd})/\text{Wd} \times 100$$

Mechanical characterization of the gellan gum spongy-like hydrogels

An INSTRON 5543 (Instron Int. Ltd., USA) was used to evaluate the mechanical properties of the wet samples. Dried structures (5 × 4 mm) were immersed in α-MEM medium for 48 h at 37 °C and then loaded on the equipment. Samples were submitted to a pre-load of 0.1 N and then tested up to 60% of strain, at a loading rate of 2 mm/min. The compressive modulus of samples was determined from the most linear part of the stress/strain curves using the secant method.

Isolation and culture of human adipose stem cells

Human adipose stem cells (hASCs) were isolated from human subcutaneous tissue samples obtained from liposuction. The samples were provided by the Hospital da Prelada (Porto, Portugal), following signed patient informed consent, under a protocol of collaboration with the 3B's Research Group, approved by the ethical committees of both institutions. The hASCs were isolated according to a standard protocol [21]. Cells were cultivated in (α-MEM) (Life Technologies, Bleiswijk, The Netherland) supplemented with 10% Fetal Bovine Serum (Life Technologies, Bleiswijk, The Netherland), 1% antibiotic/antimycotic (Life Technologies, Paisley, UK), and kept at 37 °C and 5% CO_2.

Cells at a density of 0.08×10^6 cell/structure were seeded on the top of dried polymeric networks, left for 45 min at 37 °C and 5% CO_2 to guarantee cell retention within the structure, and then cultured in α-MEM medium. For the 2D conditions, cells were cultured at a density of 1×10^4 cells/per well in 48 well plates in α-MEM (Life Technologies, Bleiswijk, The Netherland) medium. In both conditions, cells were irradiated 24 h after seeding. The irradiation was repeated for 7 consecutive days, with a 24 h interval between each irradiation, with a total of 7 irradiations per sample (Fig. 2). Experimental groups were set as: 2D-control (2D cell culture without irradiation), 2D-1 J (2D cell culture irradiated with 1 J), 2D-2 J (2D cell culture irradiated with 2 J),

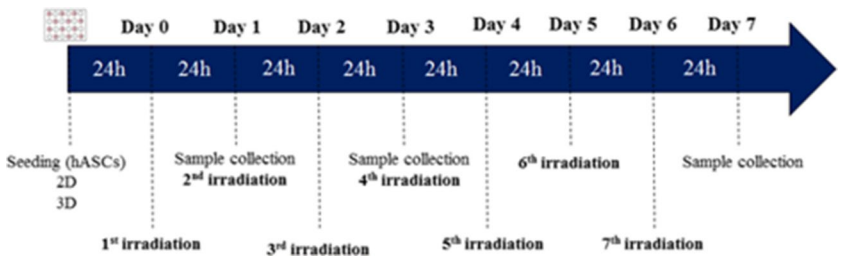

Fig. 2 Experimental design of PBM irradiation and sample collection in all groups for further analysis

2D- 6 J (2D cell culture irradiated with 6 J), 3D-control (3D cell culture without irradiation), 3D-1 J (3 D cell culture irradiated with 1 J), 3D-2 J (3D cell culture irradiated with 2 J), 3D-6 J (3D cell culture irradiated with 6 J).

Cell metabolic activity and viability

Cytotoxicity was evaluated 1, 3 and 7 days after the first PBM irradiation, by the quantification of the metabolic activity using MTS analysis (3-(4,5-dimethylthiazole-2-il)-5-(3-carboxymethoxyphenyl)-2-(4-sulfophenyl)-2H-tetrazolium) for 2D culture, and the live/dead cells by confocal microscopy for the 3D samples. A different method was used to evaluate cell viability in 3D since the diffusion of MTS reagent out of the biomaterials is compromised by the adsorption of the colorant to the biomaterials. Briefly, cells in 2D were incubated for 4 h with MTS and α-MEM culture medium without phenol red and (1:5 ratio) and the absorbance was then read at 490 nm. For 3D cultures, the cell-laden structures were incubated with a mixture of calcein (1 µg/mL, Invitrogen, USA) and propidium iodide (1 µg/mL, Invitrogen, USA) in α-MEM medium and left to incubate for 1 h in humidified atmosphere with CO_2 5% and at 37 °C. The cells were analyzed in Leica TCS SP8 confocal microscope (Leica, Germany).

Cell proliferation quantification

Cell proliferation was evaluated at 1, 3 and 7 days after the first PBM irradiation. For the 2D culture, the cells were incubated for 1 h in H2O and frozen at -80ºC prior DNA quantification. The kit Quant-IT PicoGreen dsDNA Assay Kit (Life Technologies, Scotland) was used to quantify the DNA according to the manufacturer's instructions. Briefly, DNA quantification was performed by adding 28.7 µL of sample or standard to a well of a 96-well white polystyrene plate, mixed with 100 µL of 1X Tris–EDTA buffer (10 mM Tris–HCl, 1 mM EDTA, pH 7.5) and 71.3 µL of 1X Quant-iT™ PicoGreen® reagent, all reagents from Quant-iT™ PicoGreen® dsDNA Assay Kit (Life Technologies, Scotland), and incubated for 10 min at RT. Fluorescence was read at 480 nm (excitation) and 520 (emission) in the microplate reader. For the 3D culture, cells were immunostained for the ki67 marker to infer about the proliferative state of the cells. Briefly, the structures were fixed with 400 µl of buffered formalin (Thermo Scientific, USA), incubated with 1% v/v of cold Triton-X 100 (SIGMA, Portugal) for 20 min at 4 °C for cell membrane permeabilization, followed by incubation with 2.5% v/v of horse serum (VECTASTAIN Elite ABC Kit, Vector Labs, USA) for 1 h at RT to block nonspecific antigen binding, and then with the anti-Ki67 primary antibody (1:50, Abcam, United States) at 4 ºC for 24 h. Samples were thoroughly washed with PBS prior addition of the secondary antibody (1:500, Alexa Fluor 488 – Abcam, United States) and DAPI (0.02 mg/mL, Biotium, USA overnight at 4 °C and again prior analysis with a Leica TCS SP8 confocal microscope (Leica, Germany). The number of proliferative (Ki67 positive) and the total number (DAPI stained nuclei) of cells was quantified by the software Image J to determine the % of proliferative cells in the spongy-like hydrogels.

Interleukin 8 (IL-8) quantification

The amount of IL-8 present in the supernatant of the 1, 3 and 7 day cultures after the first irradiation was quantified using the IL-8 Human ELISA kit (MyBioSource, California, USA), according to the manufacturer's instructions. High affinity microplates with monoclonal anti-cytokine were used in the experiment. A series of double dilution standard solutions was prepared according to the manufacturer's instructions. Both supernatants and standard solutions (made with recombinant cytokines at a concentration range between 15.6 pg/mL and 1000 pg/mL) were added to the well plates which were then maintained at RT for 2 h. A biotin-conjugated anti-human IL8 antibody was added to well-plates and then let to incubate on a microplate shaker at 400 rpm at RT for 2 h. Unbound biotin conjugated anti-human IL-8 antibody was removed after a wash step. Streptavidin-HRP was added to the microplate and let to incubate on a microplate shaker set at 400 rpm at RT for 1 h. After unbound Streptavidin-HRP removal during a wash step, a TMB substrate solution was added to the well-plates and incubated at RT for 10 min. The color change was measured using a spectrometer and the antigen concentration was determined by comparison to a standard curve. The sample values were obtained from an adjusted standard curve obtained at two 450 nm (excitation) and 620 nm (emission). The results were expressed in percentage (%) to control (no irradiation) for normalization.

Oxidative stress measurement

The oxidative stress was evaluated using the OxiSelect in vitro ROS/RNS assay (Cell Biolabs, USA), and the medium supernatant samples collected 1, 3 and 7 days after the first irradiation. This kit uses a 2',7'- dichlorodihydro fluorescein diacetate (DCFH) based probe. DCFHA reacts with the reactive oxygen species (ROS) generating fluorescence. Briefly, supernatants and hydrogen peroxide standard were added to wells of a 96-well plate. Subsequently, the catalyst was added to each well and then incubated 5 min at RT. DCFH solution was added to each well and further incubated at RT for 15–45 min. The samples values were obtained from an adjusted standard curve for two wavelengths, 480 nm (excitation) and 530 nm (emission). The

results were expressed in percentage (%) to control (no irradiation) for normalization.

Statistical analysis

Data are expressed as mean and standard deviation, and through descriptive methods, such as graphs and tables. Normality was evaluated with Shapiro Wilk test, and the comparison among groups was performed by variance analysis using the Two way-ANOVA test or One-way ANOVA test followed by Tukey post-test. Significant differences were set to $*p < 0.05$, and results are presented as mean ± standard deviation (S.D.). The analysis was performed using the software GraphPad Prism® 7.0 (San Diego, CA, USA). Data results from at least 3 independent experiments using triplicates.

Results

The results involving the action of PBM in different cell cultures, as well as the mod-ulation mechanisms of ROS and interleukins are presented in the sections below.

Effect of PBM on hASCs metabolic activity and viability

The effect of PBM on the viability of hASCs cultured under 2D standard conditions was evaluated by measuring their mitochondrial activity (Fig. 3A). Cell metabolic activity was not negatively affected by PBM, since mitochondrial activity was maintained similar or above the control. In fact, a significant increase of metabolic activity was evidenced after 1 and 3 doses of irradiation with a laser of 2 J, in relation to the control and a laser of 6 J.

The effect of PBM on the viability of hASCs cultured within 3D biofunctionalized GG spongy-like hydrogels was evaluated by an overall assessment of the live/dead cells (Fig. 3B). The majority of cells were viable at all timepoints, independently of the experimental groups, again confirming that PBM does not harm cells under the proposed culture conditions (Fig. 3B).

Effect of PBM in the proliferation of hASCs

The effect of PBM on the proliferation of hASCs in the 2D standard conditions was evaluated by DNA quantification (Fig. 4A). Although no differences were observed among the groups after 1 dose of irradiation, all groups that received PBM irradiation showed significantly higher DNA amount after 3 doses of irradiation than the control group (2D-1 J: 126.31%; 2D-2 J: 124.32%; 2D-6 J: 123.93%, $p < 0.05$). After 6 doses of irradiation, only cells irradiated with 1 J and 2 J showed significantly high-er DNA content than the control group (2D-1 J: 129.89% ± 19.5; 2D-2 J: 123.5% ± 20.1, $p < 0.05$).

Regarding the hASCs cultured in the 3D GG spongy-like hydrogels (Fig. 4B), immediately after the first irradiation, the amount of proliferative Ki67 positive cells was significantly higher in hASCs-laden spongy-like hydrogels irradiated with 6 J in relation to the control (3D-6 J: 168.62% ± 64.2, $p < 0.05$). After 6 doses of irradiation, all groups showed a significant increase of proliferative cells, in relation to the control (3D-1 J: 158.27% ± 37.2, 3D-2 J: 172.97% ± 13.8, 3D-6 J: 146.78% ± 14.2, $p < 0.05$).

Effect of PBM on the production of reactive oxygen species

In 2D standard conditions, no significant differences were detected for the levels of reactive oxygen species after 1 dose of irradiation, independently of the energy of irradiation (Fig. 5A). However, after 3 and 7 doses of irradiation, cells irradiated with 6 J presented a significant higher release of ROS than the control (2D-6 J—3 doses: 126.15% ± 19, 7 doses: 125.86% ± 25.5, $p < 0.05$) (Fig. 5A). This result was confirmed for cells cultured in the spongy-like hydrogels after 3 and 7 doses of irradiation of 6 J (3 doses: 119.13% ± 7.3, 7 doses: 130.9% ± 8.6, $p < 0.05$) (Fig. 5B). Moreover, hASCs-laden hydrogels irradiated with 2 J showed significant higher ROS levels after 3 and 7 doses of irradiation (3 doses: 123.2% ± 8.4, $p < 0.05$, 7 doses: 140.1% ± 6.9, $p < 0.01$) (Fig. 5B).

Effect of PBM on the production of IL-8

The effect of PBM on the release of IL-8 by hASCs was quantified by ELISA (Fig. 6). No significant differences were detected between the irradiated and control groups during all the experimental period for cells cultured in standard 2D culture conditions (Fig. 6A). However, when cells were cultured in the GG spongy-like hydrogels, the production of IL-8 was significantly diminished after 3 doses of 1 J of irradiation (46.61% ± 4.5, $p < 0.05$) and after 7 doses of any irradiation, in relation to the control (3D-1 J: 57.67% ± 9.4, 3D-2 J: 55.74% ± 14.9, 3D-6 J: 60.69% ± 4.5, $p < 0.05$) (Fig. 6B).

Discussion

PBM therapy is becoming increasingly interesting for the TERM field owed to its ability to improve MSC proliferation without altering stem cells potential [9, 10]. The "therapeutic window" that can biostimulate MSCs is known to be between 600 and 700 nm [8, 22], but the adequate PBM

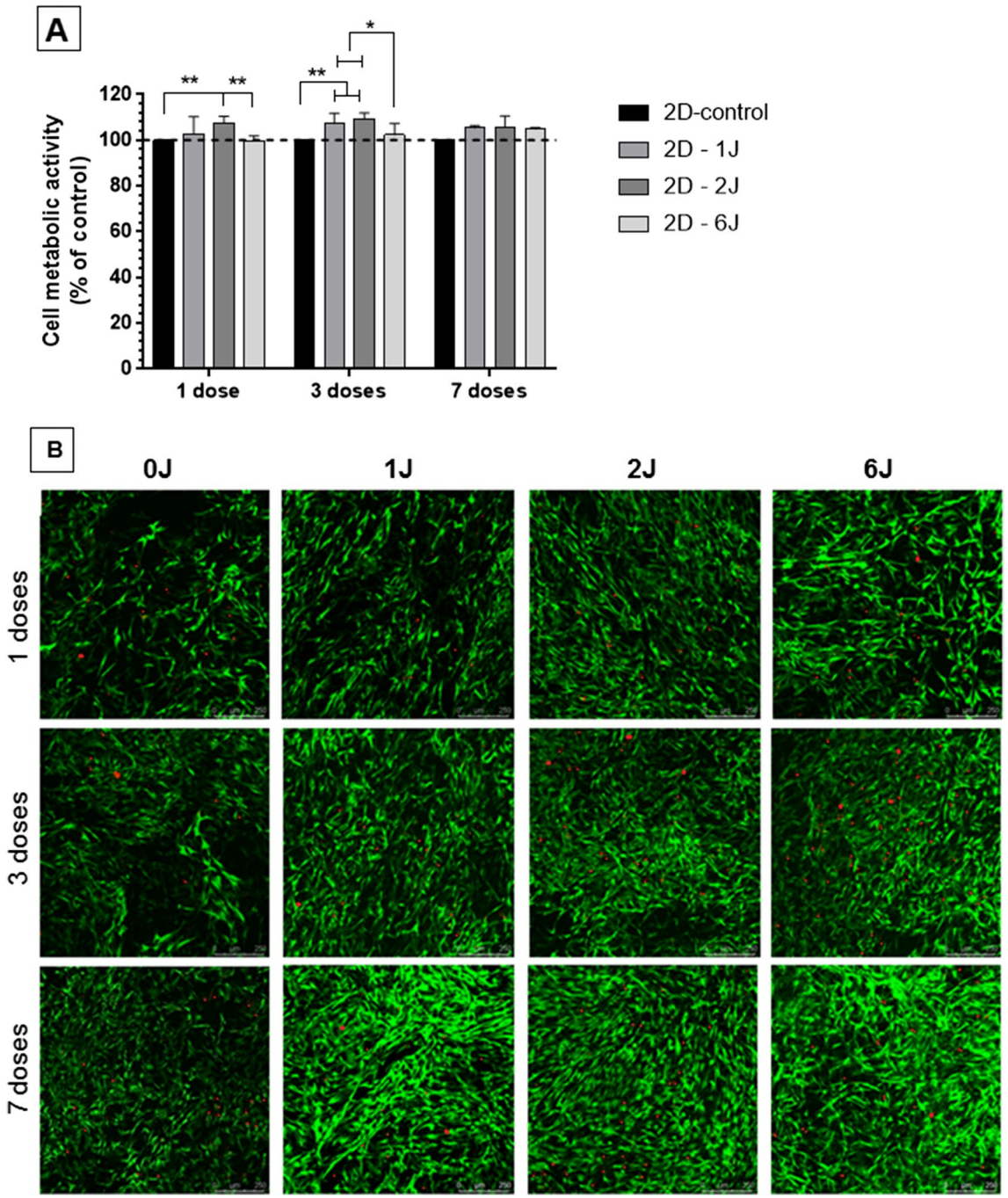

Fig. 3 Metabolic activity and viability of hASCs after PBM. **A** Metabolic activity of hASCs cultured in 2D standard conditions after irradiation with a laser of 1 J, 2 J and 6 J, in relation to the non-irradiated control (control). Data are presented as percentage (%) of 2D-0 J at day 1 for normalization and analysis of the evolution of the cultures. **B** Representative confocal microscopy images of live calcein (green) and dead propidium iodide (red) stained cells within the GG spongy-like hydrogels after irradiation with a laser of 1 J, 2 J and 6 J, at different culture timepoints (please check supplementary data for red and green images in separate). Two-way ANOVA Tukey Multiple Comparison Post-Test was used to analyze cell proliferation. Differences between the groups at each time-point are represented by * (*$p < 0.05$, **$p < 0.01$). Data results from at least 3 independent experiments using triplicates

protocols remain controversial in the literature [23]. Moreover, studies are performed in 2D culture conditions that fail to represent the in vivo environment. Thus, in this work, we aimed to explore PBM's efficacy and mode of action in hASCs cultured in 3D spongy-like hydrogels in comparison to 2D standard conditions.

The search for 3D biological models has been widely investigated in the literature, in the attempt of reducing the use of

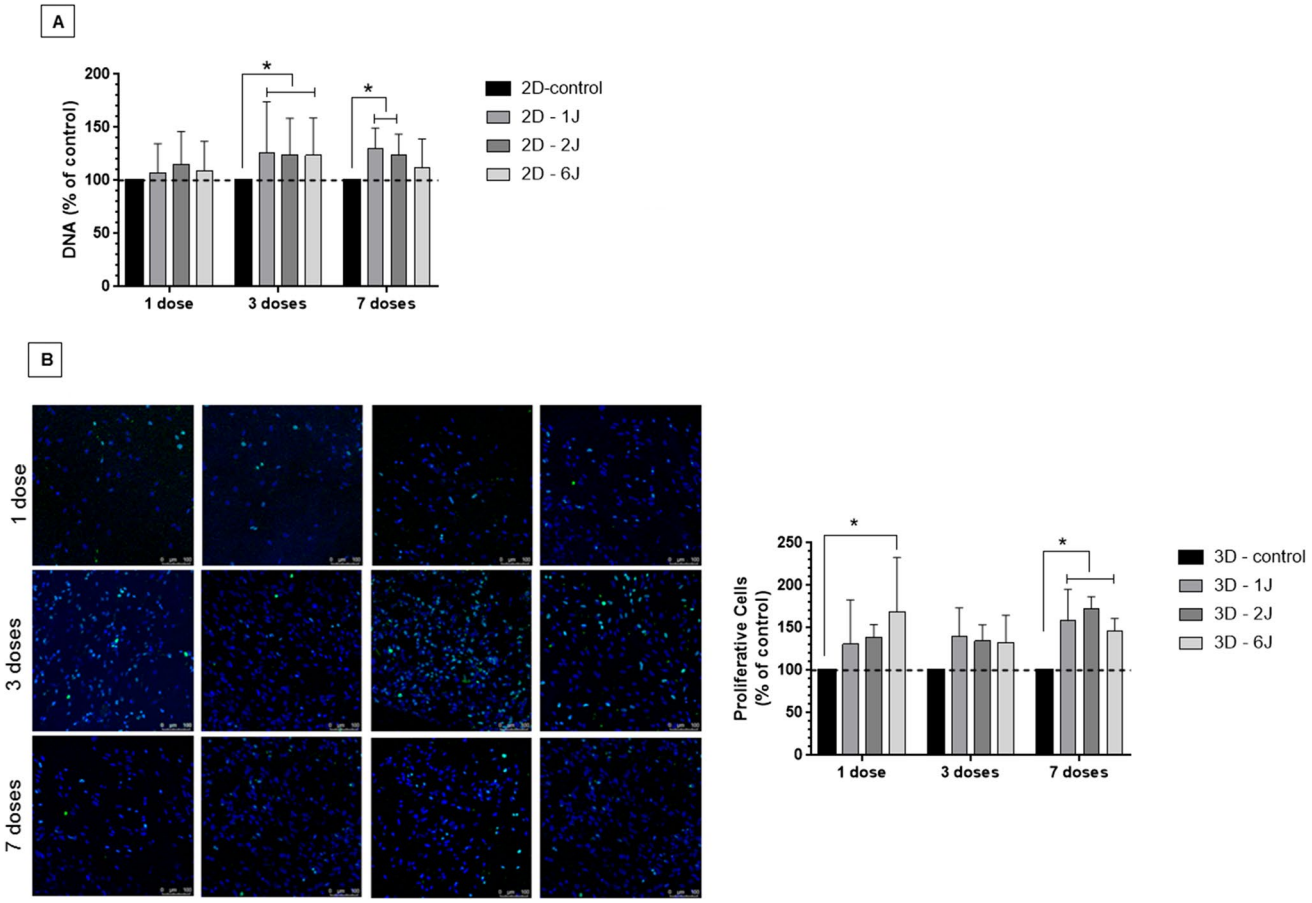

Fig. 4 Proliferation of hASCs after PBM. **A** Proliferation of hASCs in 2D standard culture conditions in the absence (control) and after irradiation with a laser of 1 J, 2 J and 6 J, determined by DNA quantification. **B** Proliferative Ki67 positive hASCs (green) in spongy-like hydrogels in the absence (3D-0 J) and after irradiation with a laser of 1 J, 2 J and 6 J, quantified from confocal microscopy images. Cell nuclei were stained with DAPI (blue). Quantitative data are presented as percentage (%) of control (control) at day 1 for normalization and analysis of the evolution of the cultures. Two-way ANOVA Tukey Multiple Comparison Post-Test was used to analyze cell proliferation. Differences between the groups at each time-point are represented by * (*$p < 0.05$). Data results from at least 3 independent experiments using triplicates

animals. Hydrogels, owed to their similarities to the microstructure and water content of the ECM, have been posed as excellent candidates. However, traditional hydrogels often fail to provide satisfactory cell adhesion sites and a sufficiently open structure to support cell migration [14]. Herein, we explored spongy-like hydrogels as 3D culture models, not only due to its ability to promote intrinsic cell adhesion and growth [20, 21], but also due to the simple and friendly cell entrapment within the precursor off-the-shelf dried polymeric structures. Moreover, spongy-like hydrogels also presented high water content, characteristic of the hydrated microenvironment of the tissues and mechanical properties in the range of soft tissues.

The effect of PBM on hASCs was different when cells were cultured in 2D and 3D conditions. None of the PBM energies negatively affected cell metabolic activity in 2D cultures and cell viability in 3D cultures. In fact, cell metabolic activity was increased in 2D conditions at certain doses and energies of irradiation. Moreover, PBM positively affected cell proliferation in 2D and the percentage of proliferative cells in 3D conditions. It was noteworthy that the cumulative 7 doses of PBM promoted cell proliferation in 2D, independently of the energy. This is in agreement with our [8] and others [9, 10, 24] previous findings showing that the application of PBM with red laser on hASCs cultured in 2D promotes cell growth, although at a different level depending on the used energy and time of exposure. Interestingly, in 3D, a significantly higher percentage of proliferative cells was detected since the first stimulation and with higher energy (6J) or after cumulative doses with lower energies (1J). To our knowledge, this was the first study that evaluated the PBM effect on MSCs proliferation in 3D cultures [25, 26]. Others explored the effect of PBM (red laser with 1 J of energy) on human dental pulp stem cells (hDPSCs) cultured in 3D cultures (agarose 3-D model) [27], but did not study PBM action on cell proliferation.

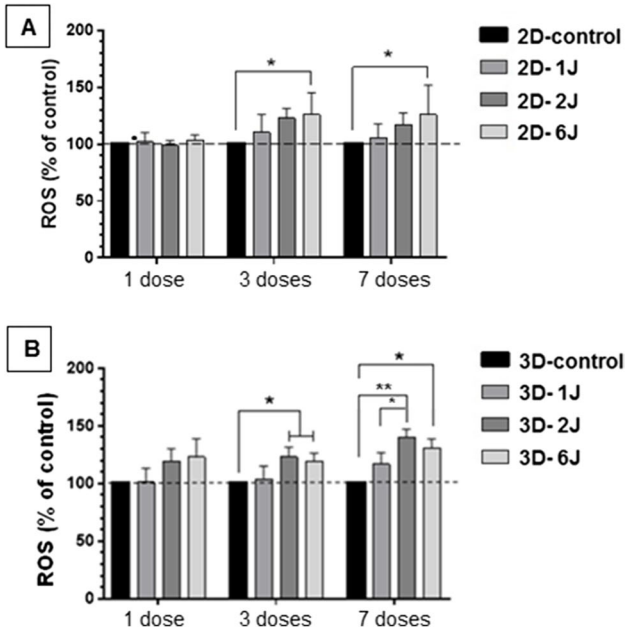

Fig. 5 Production of reactive oxygen species (ROS) after PBM. **A** Production of ROS by hASCs cultured in 2D standard culture conditions in the absence (control) and after irradiation with a laser of 1 J, 2 J and 6 J. **B** Production of ROS by hASCs cultured in spongy-like hydrogels in the absence (control) and after irradiation with a laser of 1 J, 2 J and 6 J. Quantitative data are presented as percentage (%) of control (control) at day 1 for normalization and analysis of the evolution of the cultures. Two-way ANOVA Tukey Multiple Comparison Post-Test was used to analyze cell proliferation. Differences between the groups at each time-point are represented by * (*$p < 0.05$, **$p < 0.01$). Data results from at least 3 independent experiments using triplicates

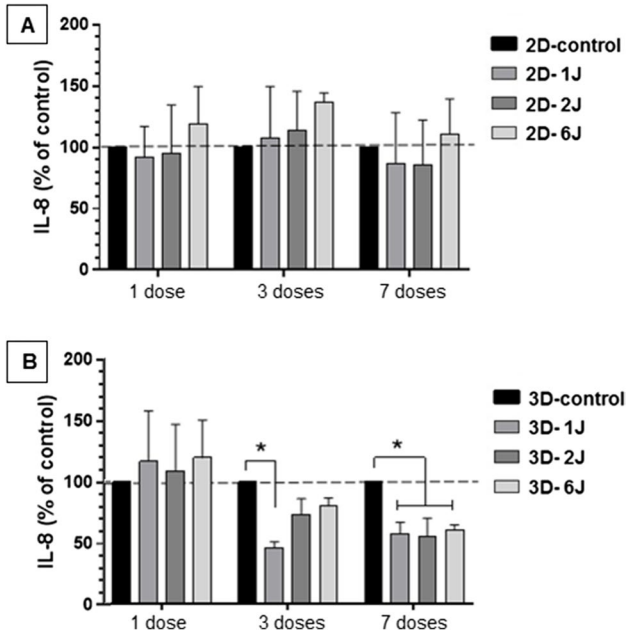

Fig. 6 Production of IL-8 after PBM. **A** Production of IL-8 by hASCs cultured in 2D standard culture conditions in the absence (control) and after irradiation with a laser of 1 J, 2 J and 6 J. **B** Production of IL-8 by hASCs cultured in spongy-like hydrogels in the absence (control) and after irradiation with a laser of 1 J, 2 J and 6 J. Quantitative data are presented as percentage (%) of control (control) at day 1 for normalization and analysis of the evolution of the cultures. Two-way ANOVA Tukey Multiple Comparison Post-Test was used to analyze cell proliferation. Differences between the groups at each time-point are represented by * (*$p < 0.05$). Data results from at least 3 independent experiments using triplicates

There are several theories that seek to explain the PBM mechanism in the cell [23, 28]. Freitas e Hamblin (2017) [29] highlighted that the absorption of light by mitochondrial cytochrome c oxidase leads to an increase in mitochondrial membrane potential and to a short burst of ROS. This is confirmed by our and others [25, 26] studies since hASCs cultured in 2D showed an increase of ROS production 3 and 7 days post-irradiation, significantly higher when cells were irradiated with a higher laser energy (6 J). This effect was also detected in 3D cultures even with lower energies (2 J).

It is also known that MSCs play an active role in immunomodulation [30]. Previous studies have shown that PBM modulates the secretion of anti and pro inflammatory cytokines [29, 31]. The release of IL-8, a potent chemoattractant of neutrophils [32], was not affected in 2D cultures, but was significantly reduced in 3D 3 and 7 days post-irradiation. A reduction of IL-8 mRNA levels was likewise detected in human periodontal ligament cells and human gingival fibroblasts co-stimulated with LPS and a laser with 660 nm and 8 J/cm^2 and 940 nm and 1.97 J/cm^2, respectively, in comparison to cells non-stimulated with LPS [33, 34]. This response was also attained in a 3D skin analogue irradiated with a laser with 660 nm and 4 J/cm^2 [35]. Although the secretion of other cytokines should be determined in order to understand the overall inflammatory status, these data indicate that PBM may trigger an anti-inflammatory profile on hASCs cultured in the spongy-like hydrogels.

All these data clearly demonstrated the differences of 2D and 3D culturing. These differences can be explained by innumerous factors that cannot be dissociated between them [36]. In contrast to 2D where cells present a stretched shape when cultured in flat surfaces, in 3D, cells present a natural shape morphology similar to the one observed in vivo. The mechanobiology also varies since the stiffness of the hydrogels is much softer than the rigid surface of 2D plates. Cell–cell communication is also limited to one plan in 2D, whereas in 3D, cells are able to connect with other cells in different plans. Moreover, it is important to state that cells in the core of biomaterials are generally in a hypoxic state, similar to in vivo tissues. Thus, the combination of these factors ultimately influence the response and signaling of cells in the two dissimilar 2D and 3D environments.

Conclusion

Photobiomodulation affected hASCs behavior both in 2D and 3D culture conditions, although at a different level depending on the number of doses and the level of energy used. The irradiation did not negatively affect cells metabolic activity in 2D nor cell viability in 3D. In fact, cell metabolic activity was significantly improved with irradiation in 2D. While a single irradiation dose was sufficient to trigger hASCs proliferation in 3D culture conditions, multiple doses were needed to trigger this effect in 2D cultures. In respect to ROS production, more than 1 dose was needed to promote ROS secretion both in 2D and 3D culture conditions. Nonetheless, cells in 3D cultures were sensible to lower energies (2 J) in contrast to cells in 2D that only responded to high energies (6 J). The release of IL-8 was also distinctly affected, as cells in 3D showed a significant reduction of IL-8 release after 3 and 7 doses of irradiation, whereas no significant differences were detected in 2D. Altogether, these results indicate that hASCs present a faster and dissimilar response to PBM in a 3D environment than in 2D cultures. Moreover, 3D cell cultures seem to be an effective alternative to understand the cell mechanisms activated by PBM, due to its closer similarity to the native tissues.

Acknowledgements We thank the Fundação Amparo à Pesquisa do Estado de São Paulo (FAPESP—2015/17648-9) and FCT – Fundação para a Ciência e a Tecnologia, I.P. and, when eligible, by COMPETE 2020 FEDER funds, under the Scientific Employment Stimulus—Individual Call (CEEC Individual)—2020.01541.CEECIND/CP1600/CT0024 (LdS) for the financial support.

Authors contribution ALMA and LPS contributed to the design and implementation of the research, to the analysis of the results. ALMA, LPS, PB, REL designed and performed the experiments and analyzed the data. APM, NAP conceived the original idea, supervised, and support the project. All authors provided critical feedback and helped shape the research analysis and to the writing of the manuscript.

Data Availability Document with complete data can be made available upon request to the responsible researcher.

Declarations

Informed consent Not applicable.

Competing interest We declare no competing interest for all the authors.

References

1. Basso FG, Soares DG, Alberto C, Costa DS (2016) Low-level laser therapy in 3D cell culture model using gingival fibroblasts. Lasers Med Sci 31:973–978. https://doi.org/10.1007/s10103-016-1945-4
2. Brassolatti P, de Andrade ALM, Bossini PS, Otterço AN, Parizotto NA (2018) Evaluation of the low-level laser therapy application parameters for skin burn treatment in experimental model: a systematic review. Lasers Med Sci. https://doi.org/10.1007/s10103-018-2526-5
3. Avci P, Gupta A, Sadasivam M, Vecchio D, Pam Z, Pam N, Hamblin MR (2013) Low-level laser (light) therapy (LLLT) in skin: stimulating, healing, restoring. Semin Cutan Med Surg 32:41–52. https://doi.org/10.1016/j.biotechadv.2011.08.021.Secreted
4. Karu T (2010) Mitochondrial mechanisms of photobiomodulation in context of new data about multiple roles of ATP. Photomed Laser Surg 28:159–160. https://doi.org/10.1089/pho.2010.2789
5. Amaroli A, Ravera S, Parker S, Panfoli I, Benedicenti A, Benedicenti S (2016) 808-nm laser therapy with a flat-top handpiece photobiomodulates mitochondria activities of Paramecium primaurelia (Protozoa). Lasers Med Sci 31:741–747. https://doi.org/10.1007/s10103-016-1901-3
6. Lipovsky A, Oron U, Gedanken A, Lubart R (2013) Low-level visible light (LLVL) irradiation promotes proliferation of mesenchymal stem cells. Lasers Med Sci 28:1113–1117. https://doi.org/10.1007/s10103-012-1207-z
7. Frigo L, Favero GM, Lima HJC, Maria DA, Bjordal JM, Joensen J et al (2010) Low-level laser irradiation (InGaAlP-660 nm) increases fibroblast cell proliferation and reduces cell death in a dose-dependent manner. Photomed Laser Surg 28:151–156
8. de Andrade ALM, Luna GF, Brassolatti P, Leite MN, Parisi JR, de Oliveira Leal ÂM, Frade MAC, de Freitas AF, Parizotto NA (2018) Photobiomodulation effect on the proliferation of adipose tissue mesenchymal stem cells. Lasers Med Sci 32:1–7. https://doi.org/10.1007/s10103-018-2642-2
9. De VJA, Houreld NN, Abrahamse H (2011) Influence of low intensity laser irradiation on isolated human adipose derived stem cells over 72 hours and their differentiation potential into smooth muscle cells using retinoic acid. Stem Cell Rev 7:869–882. https://doi.org/10.1007/s12015-011-9244-8
10. Mvula B, Mathope T, Moore T, Abrahamse H (2008) The effect of low level laser irradiation on adult human adipose derived stem cells. Lasers Med Sci 23:277–282. https://doi.org/10.1007/s10103-007-0479-1
11. Tuby H, Maltz L, Oron U (2007) Low-level laser irradiation (LLLI) promotes proliferation of mesenchymal and cardiac stem cells in culture. Lasers Surg Med 39:373–378. https://doi.org/10.1002/lsm.20492
12. Hu W, Wang J, Yu C, Lan CE, Chen G, Yu H (2007) Helium – neon laser irradiation stimulates cell proliferation through photostimulatory effects in mitochondria. J Investig Dermatol 127:2048–2057. https://doi.org/10.1038/sj.jid.5700826
13. Ayuk SM, Abrahamse H, Houreld NN (2017) Photobiomodulation alters matrix protein activity in stressed fibroblast cells in vitro. J Bio 11:1–13. https://doi.org/10.1002/jbio.201700127
14. Pampaloni F, Reynaud EG, Stelzer EHK (2007) The third dimension bridges the gap between cell culture and live tissue. Nat Rev Mol Cell Biol 8:839–845
15. Edmondson R, Broglie JJ, Adcock AF, Yang L (2014) Three-dimensional cell culture systems and their applications in drug discovery and cell-based biosensors. Assay Drug Dev Techno 12:207–218. https://doi.org/10.1089/adt.2014.573
16. Paramesh V, Kaviya SR, Anuradha E, Solomon FDP (2015) 3D cell culture systems : advantages and applications. J Cell Physiol 230:16–26. https://doi.org/10.1002/jcp.24683
17. da Silva LP, Jha AK, Correlo VM, Marques AP, Reis RL, Healy KE (2018) Gellan gum hydrogels with enzyme-sensitive biodegradation and endothelial cell biorecognition sites. Adv Healthc Mater 7:1700686. https://doi.org/10.1002/adhm.201700686
18. Silva LPD, Pirraco RP, Santos TC, Novoa-Carballal R, Cerqueira MT, Reis RL, Correlo VM, Marques AP (2016) Neovascularization induced by the hyaluronic acid-based spongy-like hydrogels degradation products. ACS Appl Mater Interfaces 8:33464–33474. https://doi.org/10.1021/acsami.6b11684

19. da Silva LP, Cerqueira MT, Sousa RA, Reis RL, Correlo VM, Marques AP (2014) Engineering cell-adhesive gellan gum spongy-like hydrogels for regenerative medicine purposes. Acta Biomater 10:4787–4797. https://doi.org/10.1016/j.actbio.2014.07.009
20. Ferris C, Stevens L, Gilmore K, Mume E, Greguric I, Kirchmajer D, Wallace G, in het Panhuis M (2015) Peptide modification of purified gellan gum. J Mater Chem B 3:1106–1115
21. Cerqueira MT, Da Silva LP, Santos TC, Pirraco RP, Correlo VM, Reis RL, Marques AP (2014) Gellan gum-hyaluronic acid spongy-like hydrogels and cells from adipose tissue synergize promoting neoskin vascularization. ACS Appl Mater Interfaces 6:19668–19679. https://doi.org/10.1021/am504520j
22. Moore P, Ridgway TD, Higbee RG, Howard EW, Lucroy MD (2005) Brief report effect of wavelength on low-intensity laser irradiation-stimulated cell proliferation in vitro. Lasers Surg Med 12:8–12. https://doi.org/10.1002/lsm.20117
23. Huang Y, Sharma SK, Carroll J, Hamblin MR (2011) Biphasic dose response in low level light therapy – an update. Dose Responde 9:602–618. https://doi.org/10.2203/dose-response.11-009.Hamblin
24. Liao X, Li SH, Xie GH, Xie S, Xiao LL, Song JX, Liu HW (2018) Preconditioning with low-level laser irradiation enhances the therapeutic potential of human adipose-derived stem cells in a mouse model of photoaged skin. Photochem Photobiol 94:780–790. https://doi.org/10.1111/php.12912
25. Wang Y, Huang YY, Wang Y, Lyu P, Hamblin MR (2017) Red (660 nm) or near-infrared (810 nm) photobiomodulation stimulates, while blue (415 nm), green (540 nm) light inhibits proliferation in human adipose-derived stem cells. Sci Rep 7. https://doi.org/10.1038/s41598-017-07525-w
26. Tani A, Chellini F, Giannelli M, Nosi D, Zecchi-Orlandini S, Sassoli C (2018) Red (635 nm), near-infrared (808 nm) and violet-blue (405 nm) photobiomodulation potentiality on human osteoblasts and mesenchymal stromal cells: a morphological and molecular in vitro study. Int J Mol Sci 19. https://doi.org/10.3390/ijms19071946
27. Zaccara I, Mestieri L, Moreira M, Grecca F, Martins M, Kopper P (2018) Photobiomodulation therapy improves multilineage differentiation of dental pulp stem cells in three-dimensional culture model. J Biomed Opt 23:1–9
28. Gao X, Xing D (2009) Molecular mechanisms of cell proliferation induced by low power laser irradiation. J Biomed Sci 16:31–37. https://doi.org/10.1186/1423-0127-16-4
29. de Freitas LF, Hamblin MR (2017) Proposed mechanisms of photobiomodulation or low-level light therapy. IEEE J Sel Top Quantum Electron 22:1–37. https://doi.org/10.1109/JSTQE.2016.2561201.Proposed
30. Yagi H, Soto-Gutierrez A, Parekkadan B, Kitagawa Y, Tompkins RG, Kobayashi N, Yarmush ML (2010) Mesenchymal stem cells: Mechanisms of immunomodulation and homing. Cell Transplant 19:667–679
31. Karu TI (1987) Photobiological fundamentals of low-power laser therapy. J Quantum Electron 23:1703–1720
32. Bickel M (1993) The role of interleukin-8 in inflammation and mechanisms of regulation. J Periodontol 64:456–460
33. Harorli OT, Hatipoglu M, Erin N (2019) Effect of photobiomodulation on secretion of IL-6 and IL-8 by human gingival fibroblasts in vitro. Photobiomodulation Photomed Laser Surg 37:457–464. https://doi.org/10.1089/photob.2018.4589
34. Lee JH, Chiang MH, Chen PH, Ho ML, Lee HE, Wang YH (2018) Anti-inflammatory effects of low-level laser therapy on human periodontal ligament cells: in vitro study. Lasers Med Sci 33:469–477. https://doi.org/10.1007/s10103-017-2376-6
35. Fiorio FB, Almeida S, De MBL, Leal-junior ECP, De P (2017) Photobiomodulation therapy action in wound repair skin induced in aged rats old : time course of biomarkers inflammatory and repair. Lasers Med Sci 32:1769–1782. https://doi.org/10.1007/s10103-017-2254-2
36. Joseph JS, Malindisa ST, Ntwasa M (2018) Two-dimensional (2D) and Three-dimensional (3D) cell culturing in drug discovery. Cell Cult. https://doi.org/10.5772/INTECHOPEN.81552